

## **General Disclaimer**

### **One or more of the Following Statements may affect this Document**

- This document has been reproduced from the best copy furnished by the organizational source. It is being released in the interest of making available as much information as possible.
- This document may contain data, which exceeds the sheet parameters. It was furnished in this condition by the organizational source and is the best copy available.
- This document may contain tone-on-tone or color graphs, charts and/or pictures, which have been reproduced in black and white.
- This document is paginated as submitted by the original source.
- Portions of this document are not fully legible due to the historical nature of some of the material. However, it is the best reproduction available from the original submission.

X-621-68-375

PREPRINT

NASA TM X- 63443

# DIURNAL AND SEASONAL VARIATION OF ATMOSPHERIC ION COMPOSITION; CORRELATION WITH SOLAR ZENITH ANGLE

H. C. BRINTON  
R. A. PICKETT  
H. A. TAYLOR, JR.

OCTOBER 1968



**GODDARD SPACE FLIGHT CENTER**  
**GREENBELT, MARYLAND**

FACILITY FORM 602

N 69-17997	
(ACCESSION NUMBER)	
32	(THRU)
(PAGES)	1
NASA-TMX-63443	(CODE)
(NASA CR OR TMX OR AD NUMBER)	13
	(CATEGORY)

**X-621-68-375**  
**PREPRINT**

**DIURNAL AND SEASONAL VARIATION OF ATMOSPHERIC  
ION COMPOSITION: CORRELATION WITH  
SOLAR ZENITH ANGLE**

by

**H. C. Brinton, R. A. Pickett, and H. A. Taylor, Jr.**

**October 1968**

**Laboratory for Atmospheric and Biological Sciences  
Goddard Space Flight Center  
Greenbelt, Maryland**

PRECEDING PAGE BLANK NOT FILMED.  
DIURNAL AND SEASONAL VARIATION OF ATMOSPHERIC  
ION COMPOSITION; CORRELATION WITH  
SOLAR ZENITH ANGLE

H. C. Brinton, R. A. Pickett, and H. A. Taylor, Jr.

ABSTRACT

A global measurement of the diurnal and seasonal variations of the primary atmospheric ions in the earth's topside ionosphere between 280 and 2700 km has been made using the ion mass spectrometer on Explorer 32. Evidence of direct correlation between solar zenith angle and the low and midlatitude distributions of thermal  $H^+$ ,  $He^+$ ,  $N^+$ , and  $O^+$  was obtained as the satellite orbit plane traversed one complete diurnal cycle between June 11 and October 5, 1966. The northern midlatitude ionosphere at 1600 km, near the  $O^+ - H^+$  transition level, exhibited strong diurnal variation,  $O^+$  rising sharply at dawn to become the dominant daytime ion with a concentration of  $1 \times 10^4$  ions/cm<sup>3</sup>;  $H^+$  was dominant at night with a concentration of  $1 \times 10^4$  ions/cm<sup>3</sup>, a factor of five higher than its daytime value. The diurnal variations of  $N^+$  and  $He^+$  in this region resembled those of  $O^+$  and  $H^+$ , respectively, at reduced concentrations. Measurements at 1200 km in the geomagnetic latitude intervals 45° to 55° (summer hemisphere) and -45° to -55° (winter hemisphere) showed a strong seasonal change in the  $O^+$  and  $N^+$  diurnal distributions, but little change in  $H^+$  and  $He^+$ . In summer the  $O^+$

concentration rose rapidly at dawn, reaching  $2 \times 10^4$  ions/cm<sup>3</sup> by 0600 LT; this daytime level was maintained until dusk at 1900 LT. The winter O<sup>+</sup>, however, was maintained at this daytime level only between 1100 and 1600 LT. The N<sup>+</sup> distributions paralleled those of O<sup>+</sup>, the O<sup>+</sup>/N<sup>+</sup> ratio being about 10. Less variation was shown by H<sup>+</sup> and He<sup>+</sup>; their daytime concentrations were  $2 \times 10^3$  ions/cm<sup>3</sup> and  $7 \times 10^1$  ions/cm<sup>3</sup>, respectively, and each had a somewhat higher nighttime value. It is found, at least for midlatitudes, that the observed diurnal and seasonal variation of the O<sup>+</sup> scale height between 1000 and 1500 km is directly related to the variation of solar zenith angle.

## CONTENTS

	Page
ABSTRACT .....	iii
INTRODUCTION .....	1
INSTRUMENTATION .....	2
ORBIT AND DATA COVERAGE .....	3
RESULTS .....	4
Ion Current Data .....	4
Diurnal Variations .....	4
Computation of Sunrise and Sunset Times .....	6
DISCUSSION .....	7
Diurnal Variation Near F-max .....	7
Diurnal Variation Near the Midlatitude O <sup>+</sup> -H <sup>+</sup> Transition Level .....	9
Diurnal Variation in the Low Latitude Protonosphere .....	10
Diurnal Variation with Changing Season .....	11
Solar Zenith Angle Correlation .....	13
ACKNOWLEDGMENTS .....	15
REFERENCES .....	16
APPENDIX. CONVERSION OF ION CURRENT TO ION CONCENTRATION .	19

DIURNAL AND SEASONAL VARIATION OF ATMOSPHERIC  
ION COMPOSITION; CORRELATION WITH  
SOLAR ZENITH ANGLE

INTRODUCTION

The ion spectrometer on Explorer 32 has provided the first global measurement of the diurnal and seasonal variations of the primary thermal ions in the topside ionosphere. This paper describes primarily the variations observed at low and midlatitudes and presents evidence of a direct relationship between solar zenith angle and the ion composition.

Explorer 32 (Atmospheric Explorer-B) was launched on May 25, 1966, into an orbit with an inclination of  $64.7^\circ$ , perigee of 277 km, and apogee of 2725 km. The spacecraft, a sealed stainless steel sphere 35 inches in diameter, carried an equator-mounted Bennett radio-frequency mass spectrometer which measured thermal positive ions in the mass range 12 to 19 amu, and 1 and 4 amu. The experiment complement also included instruments to measure electron density and temperature, neutral composition, and total neutral density. The useful satellite lifetime was approximately ten months, throughout which the ion spectrometer obtained high resolution data during nearly 8000 four minute turn-ons. The orbit of the satellite permitted observation of the diurnal behavior of the atmosphere under constant latitude-altitude conditions. The data presented here were obtained during the first complete diurnal cycle after proper orientation

of the spacecraft and final adjustment of the experiment voltages were achieved; the time interval covered was June 11 to October 5, 1966.

## INSTRUMENTATION

The Bennett ion spectrometer was similar in design to those flown on the OGO satellite series and in several rocket payloads. Since the basic instrument and theory of operation have been described in the literature [Taylor et al., 1963, 1965], only the technical details particular to this mission will be noted here. The spectrometer sensor consisted of a 5-3 cycle ceramic tube with 5 mm grid spacing and an external guard ring assembly. Two rf frequencies, 3.7 MHz and 9.0 MHz, were used with a trapezoidal-shaped sweep voltage to cover the ion mass range 12 to 19 amu, and 1 and 4 amu. An experiment turn-on consisted of one complete mass scan in 208 seconds, followed by recycling of the sweep voltage and a second measurement of the high mass range. The stopping potential ( $V_s$ ) and the guard ring potential ( $G_1$ ) controlled the sensitivity of the spectrometer; each voltage was commandable from the ground but all data presented here were obtained at a constant  $V_s$  and with  $G_1$  at satellite skin potential. The ion current reaching the spectrometer collector was measured by a series of five decade amplifiers with a particle sensitivity range of approximately  $10^1$  to  $10^6$  ions/cm<sup>3</sup>. An automatic calibrator functioned once during each turn-on to supply two known signals to the amplifier system and to

the sweep monitor; amplifier characteristics were calculated from the response to these pulses.

The spectrometer tube was mounted on the equator of the satellite as shown in Figure 1. The spacecraft spin period and attitude were magnetically controlled, the spin axis being maintained approximately normal to the orbit plane, thereby aligning the spectrometer orifice with the satellite velocity vector once each rotation. The spin rate was  $29 \pm 1$  rpm. Since the mass range was scanned slowly compared to the spin period, each peak in the ion spectrum was modulated at the spin frequency, with ion current maxima occurring when the angle between the spectrometer axis and the velocity vector was minimum. The data presented here were obtained when this angle was less than  $10^\circ$ , as determined by onboard magnetic and optical aspect sensors.

#### ORBIT AND DATA COVERAGE

The sum of the satellite orbit plane rotation ( $\approx 2^\circ/\text{day}$ ) and the motion of the earth about the sun ( $\approx 1^\circ/\text{day}$ ) caused the orbit to traverse a complete diurnal cycle in slightly less than four months. Figure 2 shows the region of data coverage during the first diurnal cycle, from June 11 to October 5, 1966. The apparent spread of the orbit is caused both by the slow movement of perigee from  $41^\circ$  to  $20^\circ$  north (geographic) latitude during this period, and by the fact that the horizontal coordinate is geomagnetic latitude. The data were acquired in real-time by thirteen ground stations and in remote areas by the spacecraft tape recorder.

## RESULTS

### Ion Current Data

Figure 3 is a photograph of the strip chart record of an experiment turn-on recorded at Johannesburg, South Africa, on August 17, 1966. The mean local time of the data is 1315 hours and during the turn-on the satellite altitude decreased from 1100 to 840 km. This record is typical of the data obtained throughout the satellite lifetime and shows spin-modulated peaks of the four ions detected: atomic oxygen ( $O^+$ ) at 16 amu, atomic nitrogen ( $N^+$ ) at 14 amu, atomic hydrogen ( $H^+$ ) at 1 amu, and helium ( $He^+$ ) at 4 amu. The degree of modulation of  $H^+$  is smaller than that of the heavier ions, due both to its lower kinetic energy with respect to the moving spacecraft and to its higher thermal velocity. The atomic oxygen isotope at 18 amu was observed whenever the abundance of the primary isotope at 16 amu was sufficiently high, the  $18^+/16^+$  ratio being approximately 0.001, near the neutral particle abundance ratio at the earth's surface.

The conversion of measured ion current to ambient ion concentration considered instrument and environment parameters and the simultaneous measurements of electron density by the companion electrostatic probe experiment. The conversion technique is described in the Appendix.

### Diurnal Variations

The diurnal variation of ionospheric composition has been investigated at a number of locations in the region of data coverage depicted in Figure 2. Data from each of the boxed areas will be discussed.

Figure 4 illustrates the diurnal variation of  $O^+$  and  $N^+$ , the dominant ions detected near satellite perigee. The altitude range of the data is 270-320 km and the geomagnetic latitude range is  $40^\circ$  to  $50^\circ$ . At the beginning of the diurnal cycle, June 1966, data in this region were obtained near 0600 LT. The local time of the data obtained on each successive day decreased by approximately 12 minutes, and by October 1966 the first diurnal cycle was completed. Relatively low concentrations of  $H^+$  ( $10^2 - 10^3$  ions/cm<sup>3</sup>) were also detected in this region throughout the diurnal cycle, but scatter in the data made definition of any local time dependence difficult. It is clear, however, that the amplitude of the  $H^+$  diurnal variation was less than a factor of three. Because of the scatter, attributable to the steep gradient in  $H^+$  concentration at perigee altitude, these data are not shown. The concentration of  $He^+$  in this region was always below 5 ions/cm<sup>3</sup>, the spectrometer limit of sensitivity for this ion.

The ion composition at higher altitudes exhibited a strong dependence on local time, as shown by Figure 5. Here the altitude range is 1500-1700 km and the geomagnetic latitude interval  $35^\circ$  to  $45^\circ$ . Note that at night the concentrations of  $O^+$  and  $N^+$  fell below the limit of sensitivity.

At mid and low latitudes  $H^+$  was dominant throughout the day at satellite apogee. The diurnal distributions of  $H^+$  and  $He^+$  are shown in Figure 6, where the altitude window is 2650-2750 km and the latitude range  $-10^\circ$  to  $-20^\circ$ . The concentrations of  $C^+$  and  $N^+$  were below the limit of sensitivity,  $5 \times 10^1$  ions/cm<sup>3</sup>, with the exception that  $O^+$  was observed as high as  $2 \times 10^2$  ions/cm<sup>3</sup> at midday.

A comparison of the diurnal variations observed at different geomagnetic latitudes and seasons may be made using Figure 7, in which data obtained in the altitude range 700-900 km between 60° and 70° north latitude (summer) are displayed with data obtained at the same altitude in the southern (winter) hemisphere between -20° and -30°. The difference in diurnal variation between the two regions is attributed primarily to season. A more precise analysis of the variation of diurnal behavior with season can be made using Figure 8. These data were obtained in the altitude range 1100-1300 km, between 45° and 55° north latitude, and in the same altitude interval in the southern hemisphere between -45° and -55°. The symmetry of these regions about the geomagnetic equator removes effects with simple latitude dependence and permits an evaluation of the diurnal profiles in terms of seasonal difference. We shall return to this analysis in a later section.

#### Computation of Sunrise and Sunset Times

In studying the variation of ionospheric composition and concentration with local time and season we found it useful to correlate ionospheric behavior with solar zenith angle and the times of sunrise and sunset at the location of the measurement. Following the notation of Colin and Myers [1966] the solar zenith angle  $\chi$  is given by

$$\cos \chi = \sin \delta \sin L + \cos \delta \cos L \cos LHA \quad , \quad (1)$$

where  $\delta$  is the solar declination,  $L$  is the geographic latitude of the observer,

and LHA is the local hour angle of the sun. The LHA, and hence the local time, of sunrise or sunset at any altitude may be computed using (1), the value of  $\chi$  at these times being given by

$$\cos \chi = - \left[ 1 - \left( \frac{a+S}{a+H} \right)^2 \right]^{1/2} \quad (2)$$

In this expression ( $a$ ) is the radius of the earth,  $H$  is altitude above the surface, and  $S$  is the "screening height" bounding the major absorbing regions of the lower atmosphere. Consideration of the screening height facilitates defining the times of sunrise and sunset at a given altitude in terms of the arrival of solar wavelengths responsible for ion production and heating. In our calculations we have assumed  $S = 30$  km [Mitra, 1952].

## DISCUSSION

### Diurnal Variation Near F-max

The data in Figure 4, obtained between 270 and 320 km, show that the mid-latitude  $O^+$  concentration increased only slightly during the day, while the midday concentration of  $N^+$  was 50 times its midnight value. The altitude range of the data coincides with the  $F_2$  maximum for  $O^+$ , where transport mechanisms are important in maintaining a relatively stable concentration throughout the day [Hanson and Patterson, 1964; Kohl and King, 1967]. Our altitude profiles of  $N^+$ , however, show that its maximum lies above 300 km and thus the diurnal variation of  $N^+$  in Figure 4 is controlled by chemical equilibrium reactions involving

the neutral atmosphere. At night, when production by photoionization ceases, the  $N^+$  concentration is depleted by the loss process  $N^+ + O_2 \rightarrow O + NO^+$  [Bauer, 1966]; the data demonstrate the effectiveness of this reaction.

The  $N^+$  concentration at 300 km (Figure 4) begins to rise approximately one hour before sunrise occurs at this altitude at the location of the measurement (Equation 1) and about 1½ hours before sunrise occurs at 170 km, the approximate altitude at which the ion production rate due to solar radiation and photoelectrons is highest. Bauer [1966] has pointed out that near 300 km a transition occurs from the region below, where  $N^+$  is produced chiefly by direct photoionization of N, to a region where the dissociative charge transfer reaction  $He^+ + N_2 \rightarrow He + N^+ + N$  is both the most important source of  $N^+$  and the primary chemical loss process for  $He^+$ . It is possible that both the observed low  $He^+$  concentration ( $< 5$  ions/cm<sup>3</sup>) and the predawn increase of  $N^+$  at 300 km may be explained in terms of the latter reaction.

At 300 km  $H^+$  is a minor ionic constituent in chemical equilibrium, its concentration increasing with altitude governed by the charge exchange process  $H^+ + O \rightleftharpoons H + O^+$ . The  $H^+$  concentration is given by the chemical equilibrium expression

$$n(H^+) = \frac{9}{8} \frac{n(H)}{n(O)} n(O^+) \quad (3)$$

[Hanson and Ortenburger, 1961]. Since neutral atmosphere models for appropriate solar activity ( $F_{10.7} = 100$ ) predict a decrease in the ratio  $n(H)/n(O)$  at

300 km by a factor of two [COSPAR, 1965] to four [Jacchia, 1964] between midnight and midday, and our data show an increase in  $n(O^+)$  by approximately the same factor, it follows that little diurnal variation of  $n(H^+)$  should be expected in this altitude range, as substantiated by our results.

#### Diurnal Variation Near the Midlatitude $O^+$ - $H^+$ Transition Level

The strong variation with local time of the midlatitude ion composition at 1600 km is shown in Figure 5. In this region the mean ion mass varied from 13.0 amu at midday, when  $O^+$  was the dominant ion, to 1.1 amu at midnight, when the composition was almost pure  $H^+$ . The nighttime concentrations of  $O^+$  and  $N^+$  were below the spectrometer limit of sensitivity, approximately  $3 \times 10^1$  ions/cm<sup>3</sup>. Sunrise at an altitude of 170 km occurred at about 0400 LT; this caused an increase in charged particle temperature, leading to a rapid rise of  $O^+$  and  $N^+$  in the 1600 km region. The relatively constant daytime concentrations of these ions were reached within two hours after sunrise. It should be noted that sunlight illuminates the 1600 km region at this latitude and season continuously, and that the observed dramatic changes in the ion composition must therefore originate in the lower ionosphere. Accompanying the decrease of  $O^+$  and  $N^+$  at dusk was an increase in  $H^+$ ; the nighttime enhancement of this ion is likely attributable to both a downward flux of protons from the protonosphere [Mayr, 1968] and to a nocturnal  $H^+$  increase in the chemical equilibrium region near 450 km, the latter caused (through relation (3)) by the greater nighttime depletion of O relative to  $O^+$  in this region as suggested by Mayr

et al. [1967]. The similarity between the diurnal behavior of  $\text{He}^+$  and  $\text{H}^+$  may be an effect of thermal diffusion, a mechanism suggested by Walker [1967] as important in reducing the difference between  $\text{H}^+$  and  $\text{He}^+$  concentration gradients in the topside ionosphere.

Data obtained in the altitude range of the orbit in the northern hemisphere between  $30^\circ$  and  $50^\circ$  reveal a daytime  $\text{O}^+$ - $\text{H}^+$  transition level of 2000 km, the concentration of both ions at that level being approximately  $5 \times 10^3$  ions/cm<sup>3</sup>. The corresponding nighttime transition altitude is 900 km, both  $\text{O}^+$  and  $\text{H}^+$  having concentrations at that level of  $1 \times 10^4$  ions/cm<sup>3</sup>. Mayr et al. [1967] have investigated the diurnal behavior of the  $\text{O}^+$ - $\text{H}^+$  transition height by solving simultaneously the energy continuity equation and the particle continuity equations for  $\text{H}^+$  and  $\text{O}^+$ . This steady state calculation reveals that the nighttime decrease of the transition level at midlatitudes is about equally influenced by the diurnal variations of electron temperature and neutral oxygen concentration. In extending this analysis to consider the dynamic case, Mayr [1968] has shown that the effect of field-aligned  $\text{H}^+$  and  $\text{O}^+$  fluxes is to increase the amplitude of the diurnal variation of the transition level.

#### Diurnal Variation in the Low Latitude Protonosphere

The dominant constituent of the low latitude ionosphere at 2700 km was  $\text{H}^+$ , with a nearly constant concentration throughout the day (Figure 6). The ratio of  $\text{H}^+$  to  $\text{He}^+$  was approximately 100, in agreement with observations over the altitude range 2000-30,000 km by the ion spectrometers on OGO 1

[Taylor et al., 1965; Brinton et al., 1968] and OGO 3 [Taylor et al., 1968a]. We are not certain whether the behavior of  $\text{He}^+$  represents a true diurnal variation, or whether it reflects ionospheric changes which occurred over the four month period of the data. Its apparent slow daytime increase, however, seems consistent with the prediction by McElroy [1965] that under conditions of low solar activity  $\text{He}^+$  may exhibit significant diurnal variation, with lower concentrations at night, and equilibrium time in excess of seven hours. The period of observation was one of low, but rising solar activity, with a mean  $F_{10.7}$  of 96 in June and 109 in October. The first data in Figure 6 were obtained at 1700 LT on June 14, the local time of observation becoming progressively earlier until the diurnal cycle was completed in October.

In the latitude range of Figure 6,  $-10^\circ$  to  $-20^\circ$ , the  $\text{O}^+$  concentration was observed as high as  $2 \times 10^2$  ions/cm<sup>3</sup> between 0900 and 1400 LT; except for this midday period  $\text{O}^+$  was not measurable, as was the case for  $\text{N}^+$  throughout the day. The concentration of  $\text{O}^+$  at 2700 km was observed to increase with increasing latitude, being approximately a factor of ten higher at  $-65^\circ$  than at  $-15^\circ$ .

#### Diurnal Variation with Changing Season

The change in diurnal variation of ion composition with season for the altitude interval 700-900 km is illustrated in Figure 7, in which data obtained at two widely separated geomagnetic latitudes are displayed. In the northern (summer) hemisphere between  $60^\circ$  and  $70^\circ$  the day-night variation of  $\text{O}^+$  and  $\text{N}^+$

concentrations was less than a factor of ten; this contrasts with the behavior in the southern (winter) hemisphere between  $-20^\circ$  and  $-30^\circ$  where the variation was greater than two orders of magnitude. While we believe this difference is primarily seasonal, the high latitude distributions may also have been influenced by heating and ionizing effects associated with incoming particle fluxes in the polar region [Thomas et al., 1966]. In the summer hemisphere the sun illuminated the 170 km altitude level continuously, except for a period of less than one hour near midnight. In the winter hemisphere sunrise at 170 km occurred at 0500 LT and sunset at 1830 LT. The light ions  $H^+$  and  $He^+$  did not show a well defined diurnal variation, due partly to scatter in the data. There is, however, a difference in the average concentrations measured in the two hemispheres which we attribute primarily to the difference in absolute geomagnetic latitude of the observations. Both  $H^+$  and  $He^+$  decrease in abundance with increasing latitude, in agreement with the measurements made by the ion spectrometer on OGO 2 [Taylor et al., 1968b].

To better define the variation of ionospheric diurnal behavior with season the effects of altitude and geomagnetic latitude must first be removed from the data. In Figure 2 it may be seen that certain portions of the Explorer 32 orbit are symmetrical about the geomagnetic equator in both latitude and altitude. Data from two such symmetrical regions are shown in Figure 8; the altitude range of the data is 1100-1300 km, and the geomagnetic latitude intervals are  $45^\circ$  to  $55^\circ$  in the northern (summer) hemisphere, and  $-45^\circ$  to  $-55^\circ$  in the southern

(winter) hemisphere. The difference in diurnal behavior of  $O^+$  and  $N^+$  between the two hemispheres is seasonal, and is related to the difference in diurnal variation of the solar zenith angle at the two locations. This relationship will be discussed further in connection with Figure 9. No seasonal effect was discernible in the light ions  $H^+$  and  $He^+$ , with the exception that the  $He^+$  concentrations measured in the winter hemisphere appeared to be slightly higher than those detected in the summer hemisphere. The daytime concentrations of both  $H^+$  and  $He^+$  were generally lower than the nighttime values, in agreement with the data of Figure 5 at a comparable altitude.

#### Solar Zenith Angle Correlation

Based on a study of topside sounder data from Alouette I Chandra and Rangaswamy [1967] have pointed out the complex manner in which solar zenith angle and magnetic latitude are related to the observed diurnal and seasonal variations of electron density at 1000 km. For the data presented in Figure 8 the effects of these two variables have been separated, in that the geomagnetic latitude interval remains constant while the zenith angle varies with local time and season. The relationship between zenith angle and the diurnal and seasonal variation of  $O^+$  at 1200 km may be studied using Figure 9. The curves in the left panel are identical to those in the upper left block of Figure 8, while the curves on the right describe the variation of solar zenith angle at the locations of the  $O^+$  measurements. The zenith angle was calculated using Equation (1); the slight asymmetry of the curves is caused by the changing declination of the sun during the four month diurnal cycle.

Assuming, as before, a screening height of 30 km, sunrise and sunset at 170 km occur when the solar zenith angle is approximately  $102^\circ$ ; the local times of sunrise and sunset at the locations of the data are indicated in the figure. In the summer hemisphere latitude range the sun is below the "horizon" at night for less than seven hours, and even at 2400 LT it is below by less than  $15^\circ$ . The nighttime  $O^+$  concentration at 1200 km in the summer hemisphere is thereby maintained at a level almost an order of magnitude higher than that at the same latitude in the winter hemisphere, where night is nearly five hours longer and the sun dips below the "horizon" by more than  $60^\circ$ . For several hours following sunrise, as the solar zenith angle decreases, the  $O^+$  concentration rises. When the zenith angle reaches  $60^\circ$  the concentration levels off at a broad daytime plateau in the summer hemisphere, although the zenith angle continues to decrease, reaching  $20^\circ$  by 1200 LT. The winter hemisphere zenith angle is never less than  $60^\circ$ , resulting in a short midday plateau of  $O^+$  concentration.

The foregoing correlation between the behavior of  $O^+$  and the variation of solar zenith angle emphasizes the strong relationship between the latter and both daily and seasonal characteristics of the ionosphere. Correlation may also be demonstrated between zenith angle and observed  $O^+$  scale height in the altitude range 1000-1500 km. The variation of scale height was determined by sorting  $O^+$  measurements made during the diurnal cycle into groups having similar local time and geomagnetic latitude. Altitude profiles were constructed from the data in twenty such groups, representing local times between 0000 and

1200 LT and latitude intervals  $35^\circ$  to  $55^\circ$  and  $-35^\circ$  to  $-55^\circ$ . The scale height of each resulting  $O^+$  distribution was estimated by fitting a straight line to the altitude profile between 1000 and 1500 km, and the solar zenith angle corresponding to the time and location of each profile was calculated using Equation (1). The results are presented in Figure 10, where data from both hemispheres have been combined to show the dependence of scale height on zenith angle. At a given geographic location local time increases nonlinearly from right to left on the zenith angle axis. Thus, the midlatitude  $O^+$  scale height at night in the winter (southern) hemisphere is approximately 100 km. After sunrise, as the zenith angle decreases, the charged particle temperature rises, causing the scale height to increase rapidly and then level off at approximately 330 km for zenith angles less than  $60^\circ$ ; the latter condition exists during the day at midlatitudes in the summer (northern) hemisphere. We conclude from Figure 10 that, at least for midlatitudes, the effects of both local time and season on the  $O^+$  altitude distribution between 1000 and 1500 km are directly related to the variation of solar zenith angle.

#### ACKNOWLEDGMENTS

The authors are indebted to J. T. Coulson for his contributions to the development of the ion spectrometer, and to Dr. H. G. Mayr for helpful discussions of the data. We also wish to thank L. H. Brace for the use of his unpublished electron density data.

## REFERENCES

- Bauer, S. J., Chemical processes involving helium ions and the behavior of atomic nitrogen ions in the upper atmosphere, J. Geophys. Res., 71, 1508-1511, 1966.
- Brinton, H. C., M. W. Pharo, III, H. G. Mayr, and H. A. Taylor, Jr., Implications for ionospheric chemistry and dynamics of a direct measurement of ion composition in the F<sub>2</sub>-region, submitted to J. Geophys. Res., 1969.
- Brinton, H. C., R. A. Pickett, and H. A. Taylor, Jr., Thermal ion structure of the plasmasphere, Planet. Space Sci., 16, 899-909, 1968.
- Chandra, S. and S. Rangaswamy, Geomagnetic and solar control of ionization at 1000 km, J. Atmos. Terrest. Phys., 29, 259-265, 1967.
- Colin, L. and M. Myers, Computed times of sunrise and sunset in the ionosphere, NASA/AMES Rept. TMX-1233, Moffett Field, Calif., April 1966.
- COSPAR International Reference Atmosphere 1965, North-Holland Publishing Co., Amsterdam, 1965.
- Hanson, W. B. and I. B. Ortenburger, The coupling between the protonosphere and the normal F-region, J. Geophys. Res., 66, 1425-1435, 1961.
- Hanson, W. B. and T. N. L. Patterson, The maintenance of the nighttime F-layer, Planet. Space Sci., 12, 979-997, 1964.
- Jacchia, L. G., Static diffusion models of the upper atmosphere with empirical temperature profiles, Special Report 170, Smithsonian Institution Astrophysical Observatory, Cambridge, Mass., December, 1964.

- Kohl, H. and J. W. King, Atmospheric winds between 100 and 700 km and their effects on the ionosphere, J. Atmos. Terrest. Phys., 29, 1045-1062, 1967.
- Mayr, H. G., The dynamic coupling between F<sub>2</sub>-region and protonosphere, NASA-GSFC document X-621-68-300, 1968, submitted to Planet. Space Sci.
- Mayr, H. G., L. H. Brace, and G. S. Dunham, Ion composition and temperature in the topside ionosphere, J. Geophys. Res., 72, 4391-4403, 1967.
- McElroy, M. B., Excitation of atmospheric helium, Planet. Space Sci., 13, 403-433, 1965.
- Mitra, S. K., The upper atmosphere, second ed., (the Asiatic Monograph Series, v.V), The Asiatic Society, Calcutta, India, 1952.
- Taylor, H. A., Jr., L. H. Brace, H. C. Brinton, and C. R. Smith, Direct measurements of helium and hydrogen ion concentration and total ion density to an altitude of 940 kilometers, J. Geophys. Res., 68, 5339-5347, 1963.
- Taylor, H. A., Jr., H. C. Brinton, and M. W. Pharo, III, Contraction of the plasmasphere during geomagnetically disturbed periods, J. Geophys. Res., 73, 961-968, 1968a.
- Taylor, H. A., Jr., H. C. Brinton, M. W. Pharo, III, and N. K. Rahman, Thermal ions in the exosphere; evidence of solar and geomagnetic control, J. Geophys. Res., 73, 5521-5533, 1968b.
- Taylor, H. A., Jr., H. C. Brinton, and C. R. Smith, Positive ion composition in the magnetoionosphere obtained from the OGO-A satellite, J. Geophys. Res., 70, 5769-5781, 1965.

Thomas, J. O., M. J. Rycroft, L. Colin, and K. L. Chan, Electron density profiles in ionosphere and exosphere, Proc. NATO Advan. Study Inst., Finse, Norway, edited by Jon Frihagen, North-Holland Publishing Co., Amsterdam, 1966.

Walker, J. C. G., Thermal diffusion in the topside ionosphere, Planet. Space Sci., 15, 1151-1156, 1967.

Whipple, E. C., Jr., The ion-trap results in "Exploration of the upper atmosphere with the help of the third Soviet sputnik", Proc. IRE, 47, 2023-2024, 1959.

## APPENDIX

### CONVERSION OF ION CURRENT TO ION CONCENTRATION

To interpret measured ion current in terms of ambient particle concentration the peak value of the modulation envelope for each ion peak is used, since this current is obtained for conditions of minimum attack angle and optimum spectrometer sweep potential.

Under conditions of negative spacecraft and sensor orifice potential, small attack angle, and ion thermal velocity less than or comparable to the satellite velocity, the relationship between collected current,  $I$ , and ambient concentration,  $n_i$ , for each ion is given by

$$I = n_i e v A \alpha , \quad (4)$$

where  $e$  is the electronic charge,  $v$  is the satellite velocity,  $A$  is the spectrometer orifice area, and  $\alpha$  is the spectrometer efficiency for the particular ion, including the correction for mass discrimination within the instrument. Results from the companion electrostatic probe experiment indicate that spacecraft potential varied slightly about an average value of  $-0.7$  volts, except in regions where the ambient electron density was too low to override photoemission, which caused the satellite to go slightly positive [L. H. Brace, private communication]. Data obtained under the latter condition are not included in this paper. Although the mean thermal velocity of the atmospheric hydrogen ions may be comparable to the spacecraft velocity (6-8 km/sec), consideration of the

expanded form of (4) [Whipple, 1959] shows that the error introduced by simplifying the equation is small.

The efficiency,  $\alpha$ , is a function of incident ion energy, and may be expressed as

$$\alpha = k_1 + k_2 v^2, \quad (5)$$

where  $k_1$  and  $k_2$  are laboratory-determined constants for a particular ion species. Combining (4) and (5), the expression for the concentration of an ionic constituent becomes

$$n_i = \frac{I}{e A(k_1 v + k_2 v^3)}. \quad (6)$$

Assuming charge neutrality ( $n_e = \Sigma n_i$ ), the comparison of ion concentrations calculated using (6) with electron concentrations measured simultaneously by the electrostatic probes has indicated an apparent difference of efficiency for the measurements of mass 16 ( $O^+$ ) and mass 1 ( $H^+$ ). This difference may be an effect of mass discrimination occurring outside the spectrometer. Under certain local time and latitude conditions  $O^+$  has been observed to be strongly dominant at altitudes ranging from perigee up to 1500 km; in these cases (where  $\Sigma n_i \approx n_{O^+}$ ),  $n_e/n_i = 2.1$ . Under other conditions  $H^+$  has been observed dominant from apogee down to 800 km; in these cases (where  $\Sigma n_i \approx n_{H^+}$ ),  $n_e/n_i = 0.40$ . Assuming that the electron concentration measurement is accurate to approximately 20% [L. H. Brace, private communication], we have multiplied the right hand side of

(6) by a normalization factor; the resulting expression has been used to derive the ion concentrations reported here. The normalization factor determined for  $H^+$ , 0.40, was also used for  $He^+$ , and the factor 2.1 was used for both  $O^+$  and  $N^+$ .

Ion concentrations measured by spectrometers flown on two sounding rockets near the time of the Explorer 32 data are consistent with the satellite results. The midday concentrations of  $O^+$  and  $N^+$  measured at 300 km by the ion spectrometer on NASA 18.06 are in excellent agreement with the data in Figure 4 [M. W. Pharo, III, private communication]; NASA 18.06 was launched on August 26, 1966, from Wallops Island, Virginia, to coincide with an overflight of Explorer 32. Equally good agreement exists between the satellite data and the concentrations of  $O^+$ ,  $N^+$ , and  $H^+$  at 300 km measured by the ion spectrometer on the Geoprobe (NASA 8.25) rocket [Brinton et al., 1969]. This flight, also from Wallops Island, occurred at midday on March 2, 1966, approximately three months prior to the Explorer 32 launch.

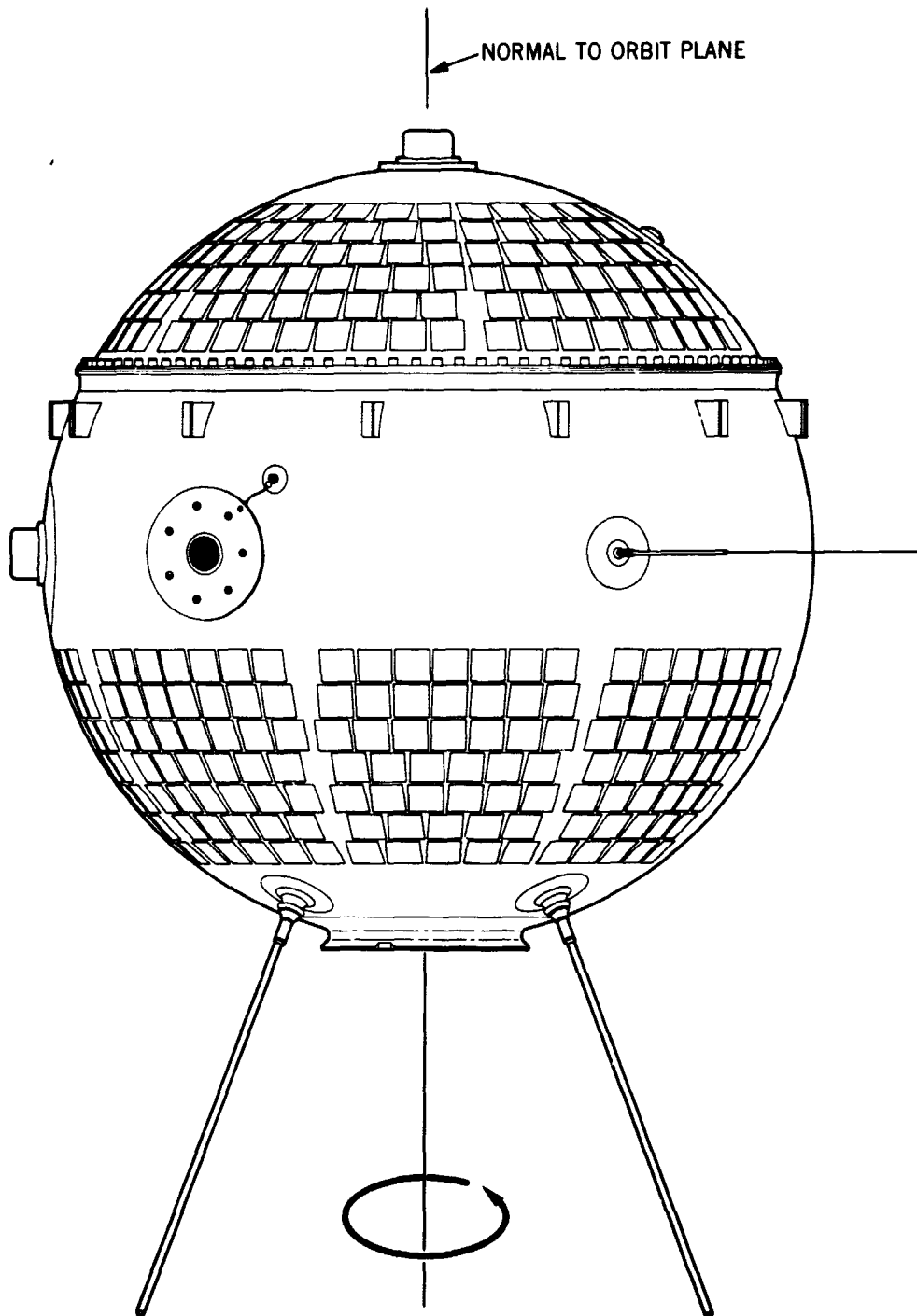


Figure 1. Explorer 32 (Atmospheric Explorer-B), showing ion mass spectrometer orifice and guard ring, and cylindrical electrostatic probe. Instruments are mounted on equator, perpendicular to spacecraft spin axis.

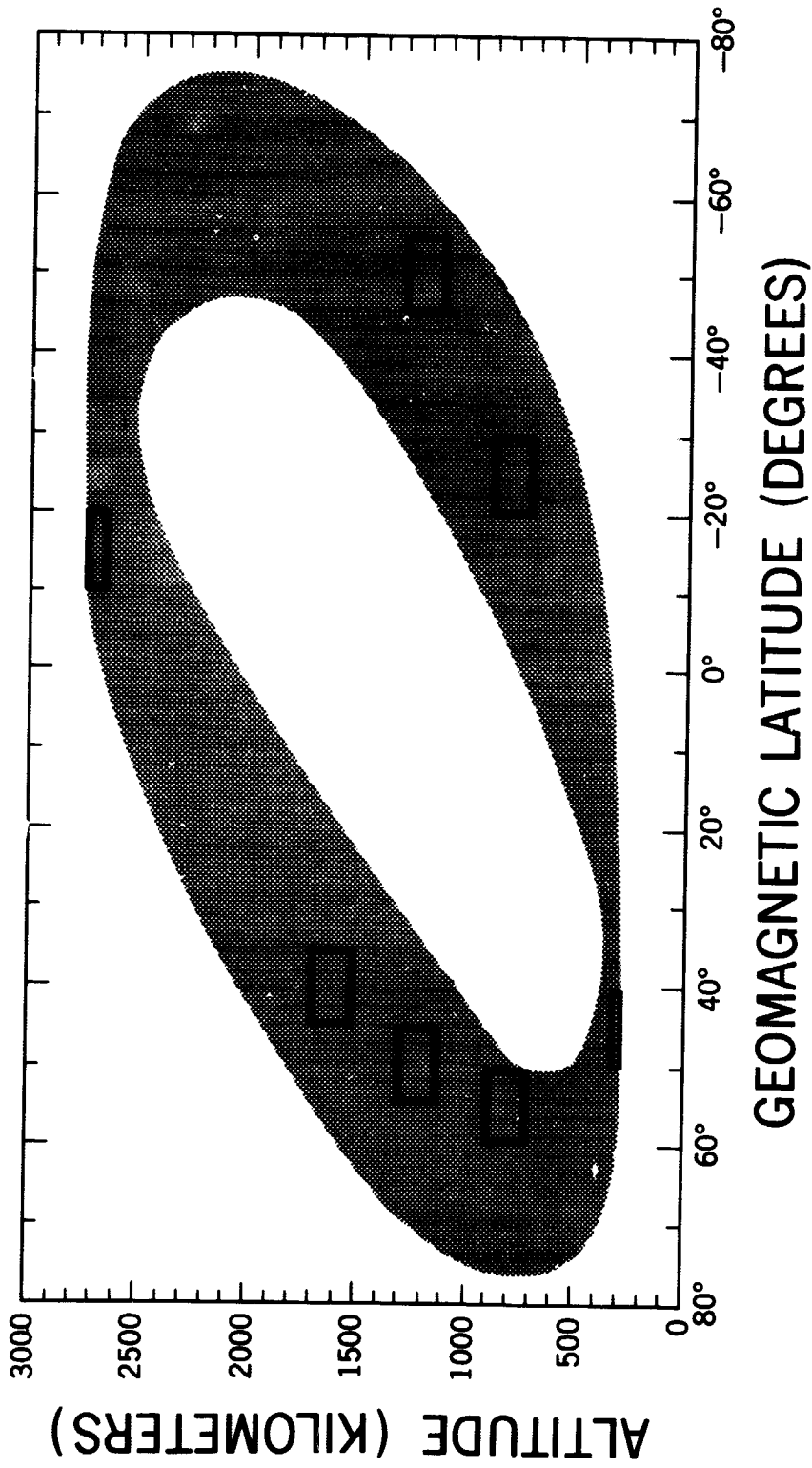


Figure 2. Region of data coverage during first diurnal cycle, June 11 to October 5, 1966.  
Data discussed in text were obtained in boxed areas.

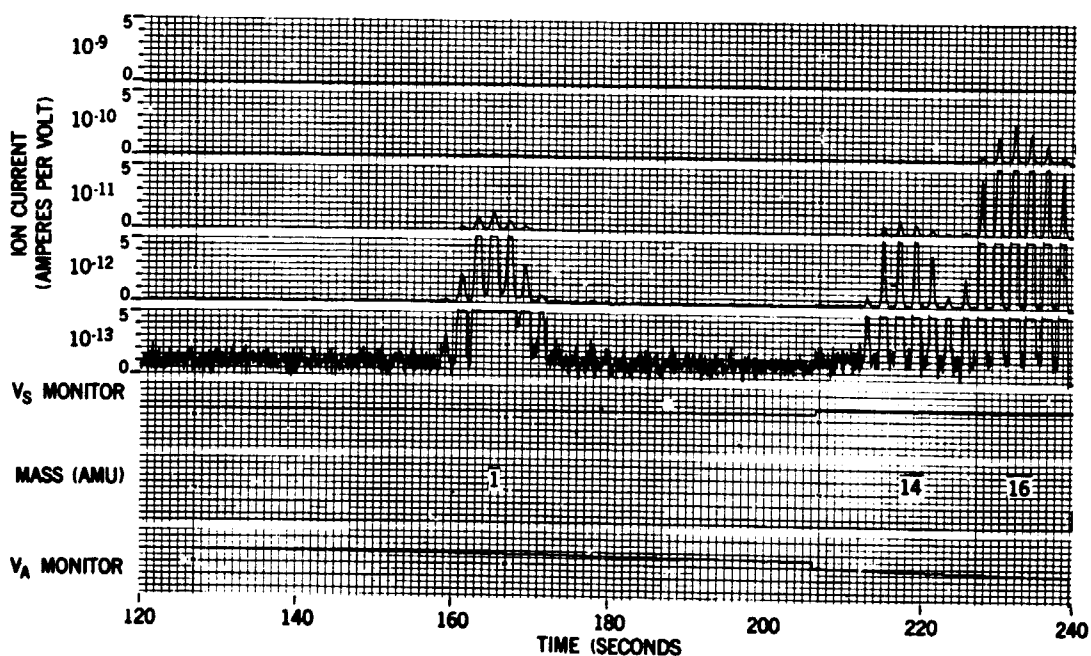
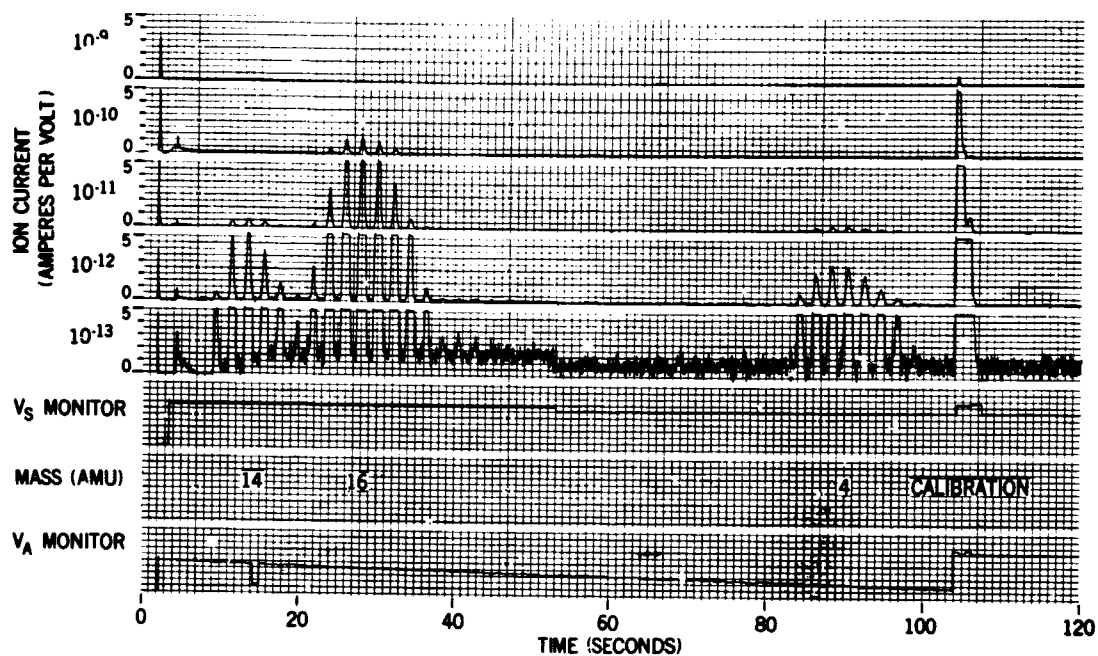


Figure 3. Typical ion spectrometer turn-on, recorded at Johannesburg; satellite was near 1000 km altitude. Spin-modulated ion current peaks and automatic amplifier calibration are shown.

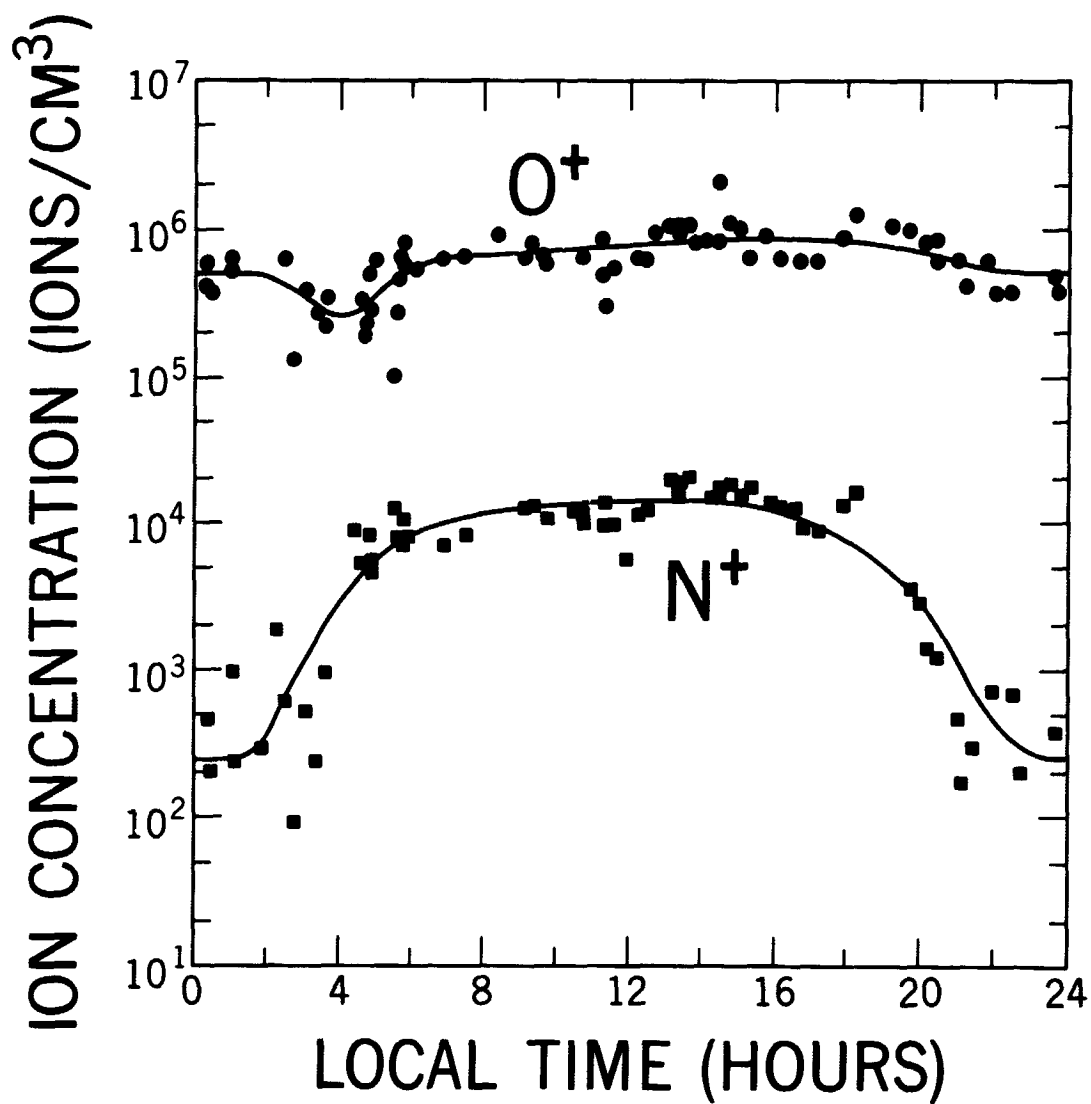


Figure 4. Diurnal variation of dominant ions near midlatitude F-max.  
 Altitude range, 270-320 km; geomagnetic latitude range, 40° to 50°; June-October, 1966.

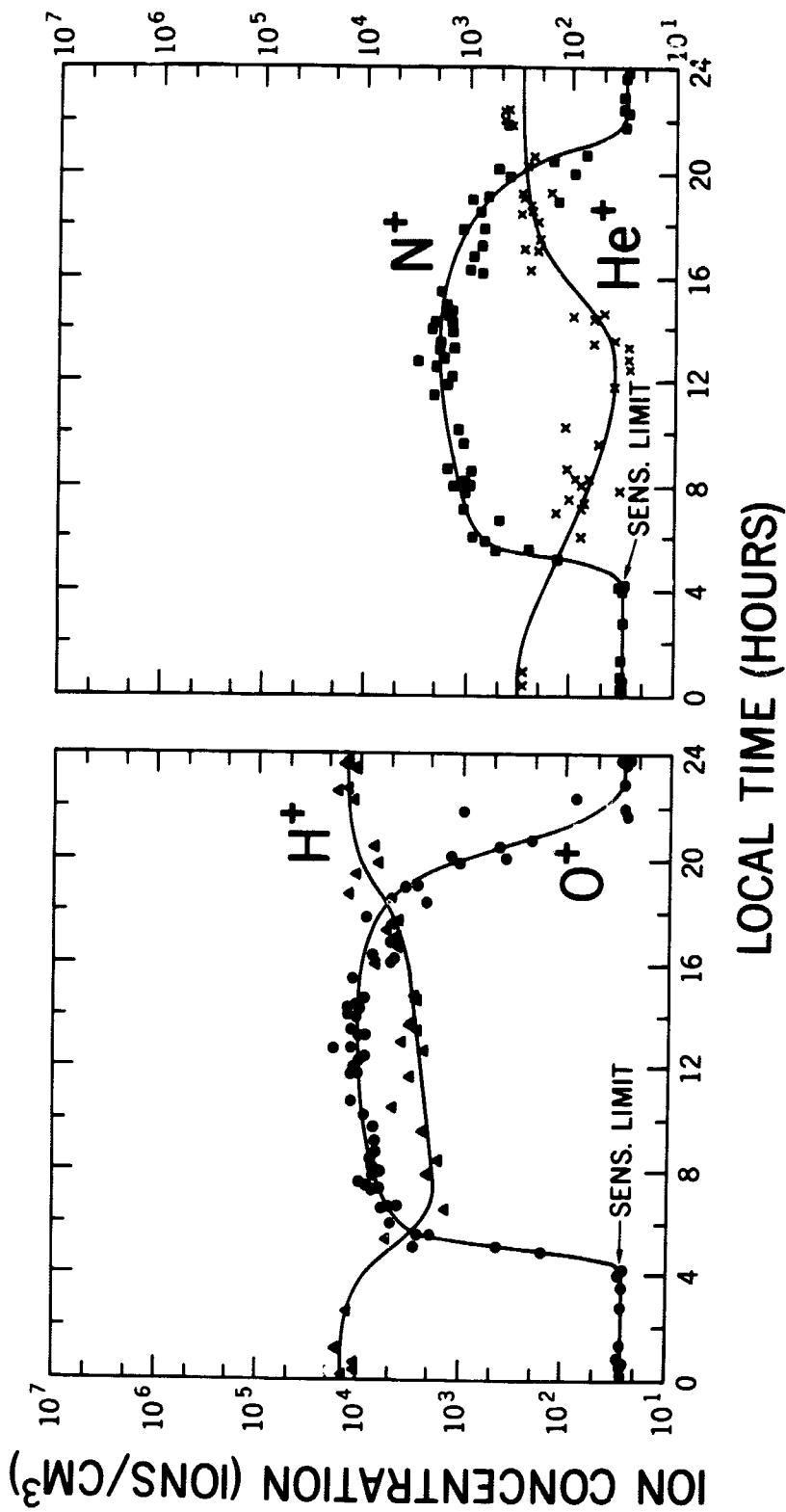


Figure 5. Diurnal variation of midlatitude ion composition near O<sup>+</sup>-H<sup>+</sup> transition level. Altitude range, 1500-1700 km; geomagnetic latitude range, 35° to 45°; June-October, 1966.

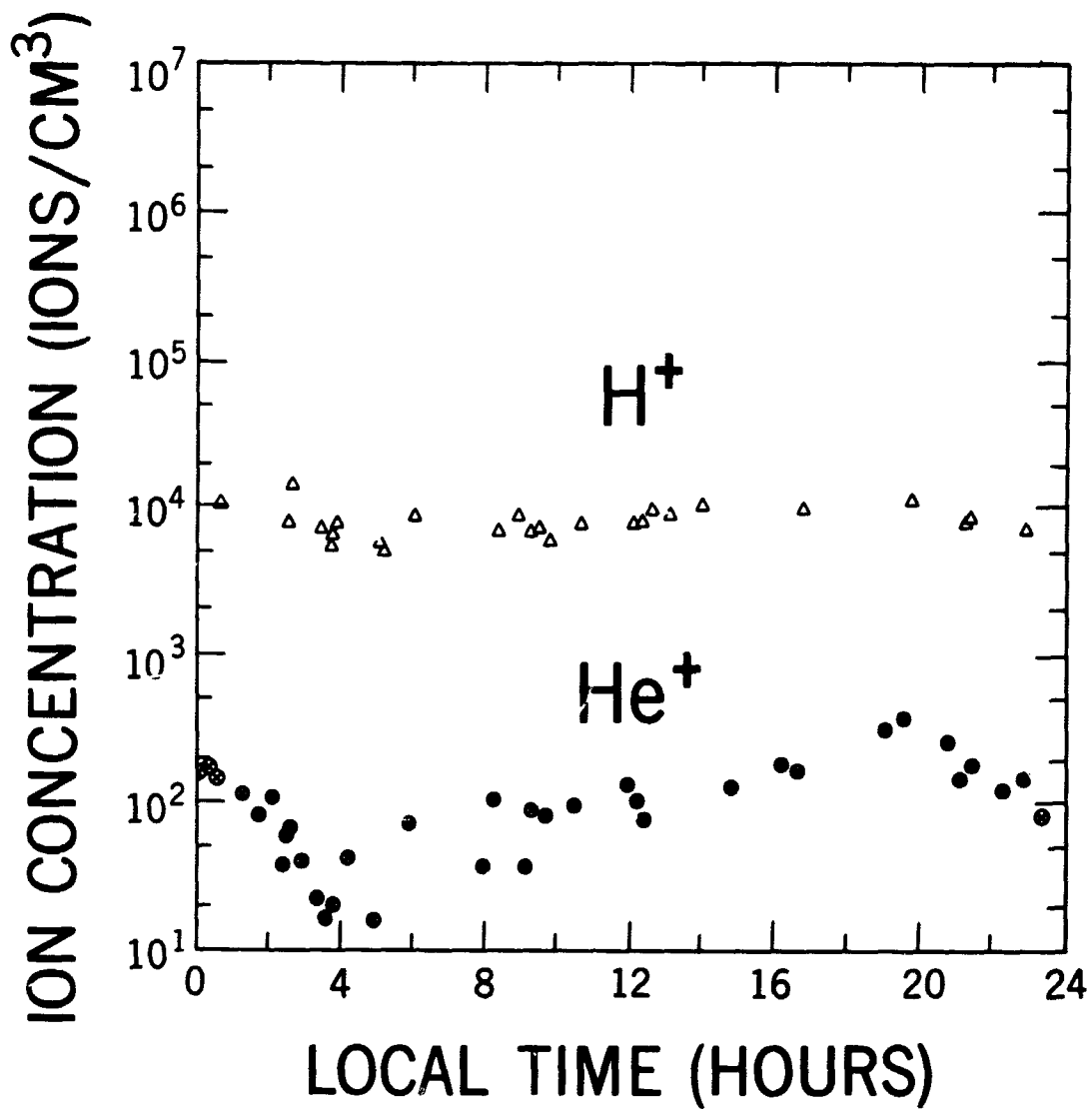


Figure 6. Diurnal variation of light ions in the low latitude protonosphere. Altitude range, 2650-2750 km; geomagnetic latitude range,  $-10^\circ$  to  $-20^\circ$ ; June-October, 1966.

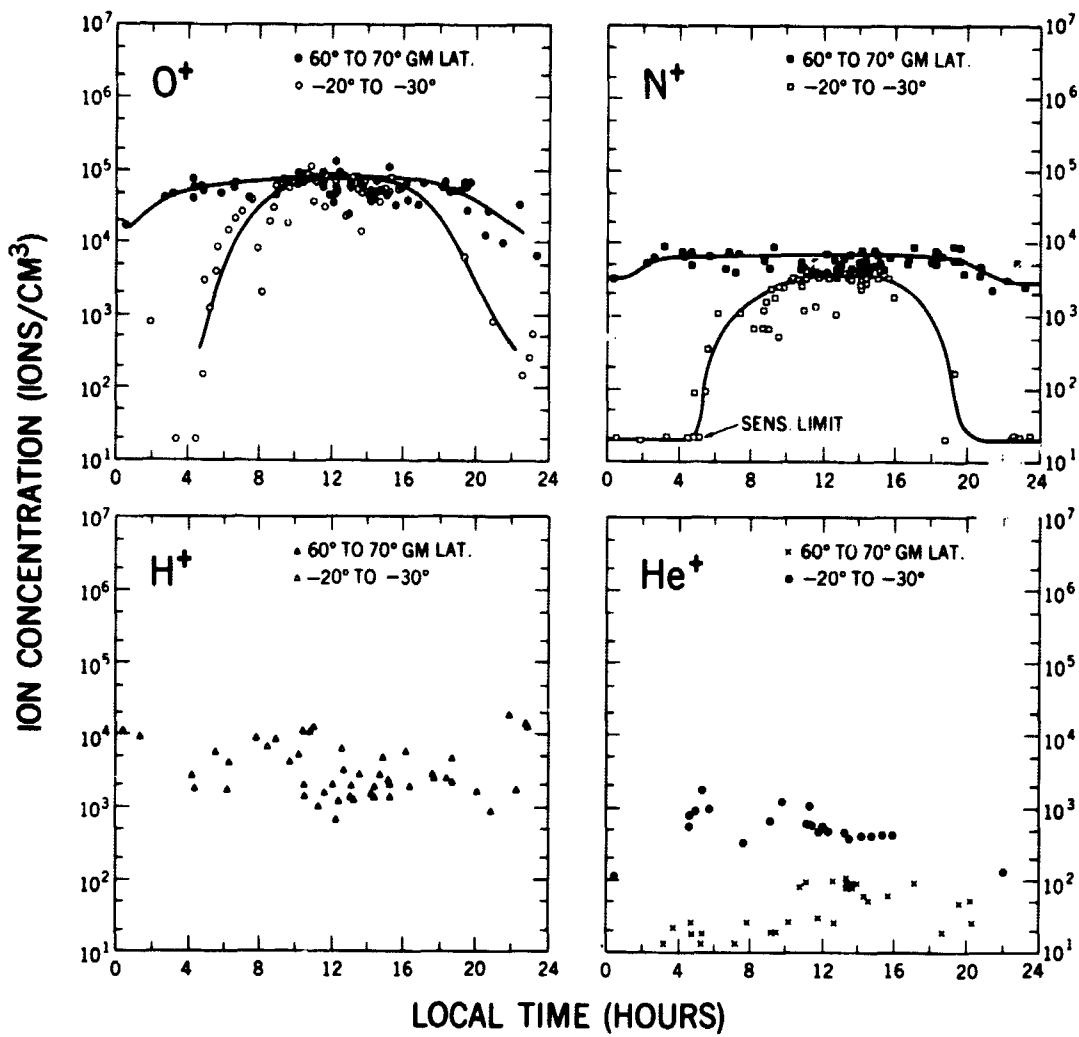


Figure 7. Variation of diurnal behavior in the altitude range 700-900km with geomagnetic latitude (June-October, 1966); the variation of O<sup>+</sup> and N<sup>+</sup> is believed to be primarily seasonal.

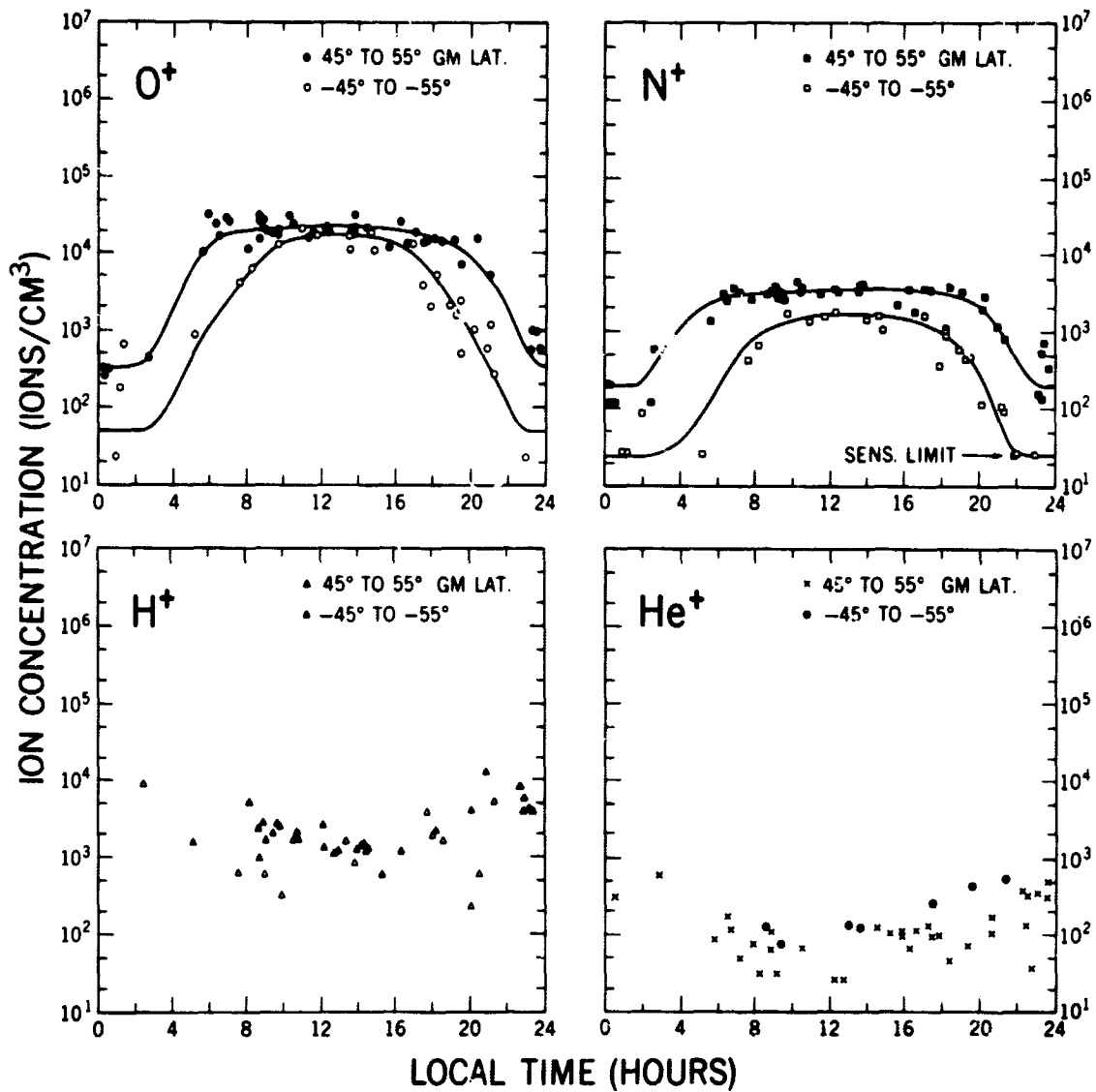


Figure 8. Variation of diurnal behavior in the altitude range 1100-1300 km between summer (northern) hemisphere and winter (southern) hemisphere. Symmetry about the geomagnetic equator removes effects with simple latitude dependence.

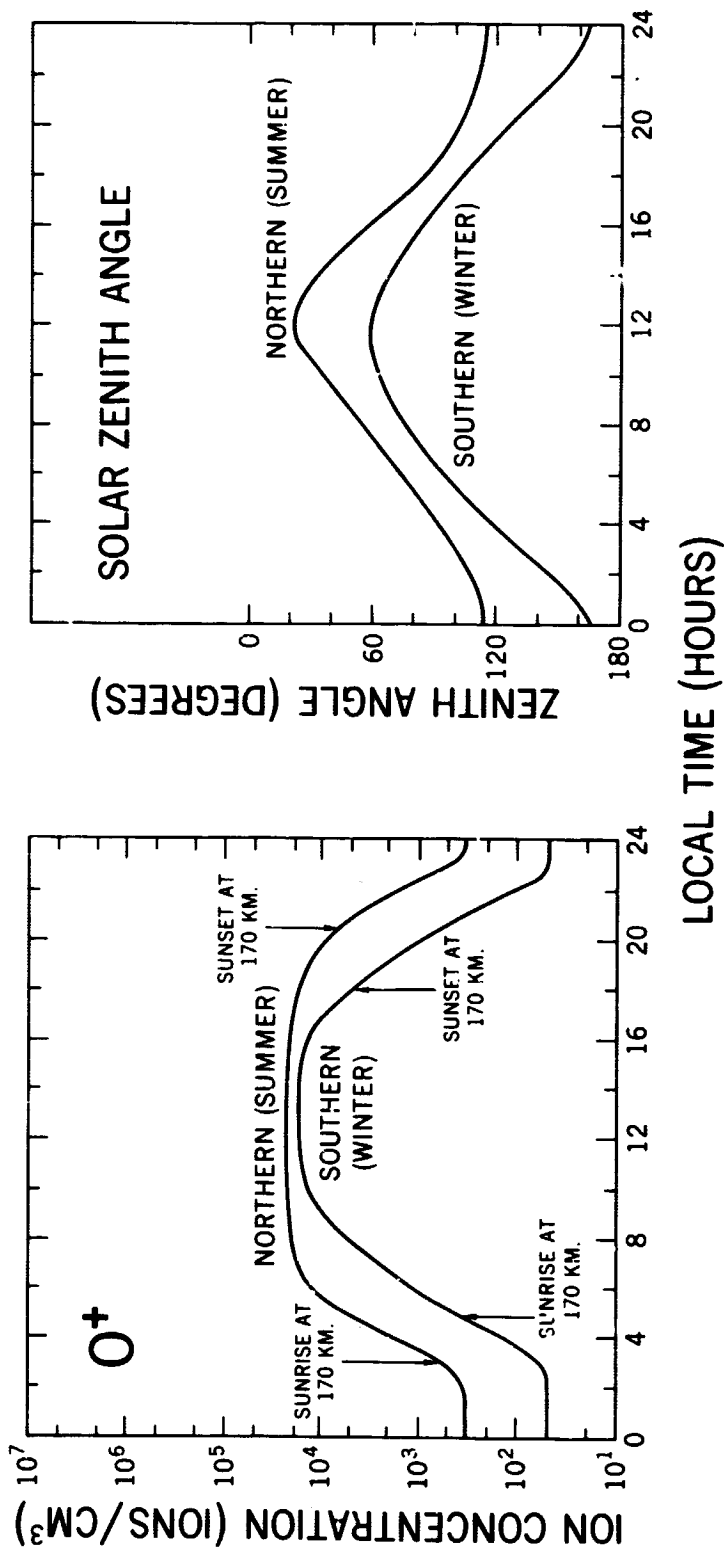


Figure 9. Observed diurnal and seasonal behavior of  $O^+$  concentration near 1200 km (from Figure 8), compared with variation of solar zenith angle at locations of  $O^+$  measurements.

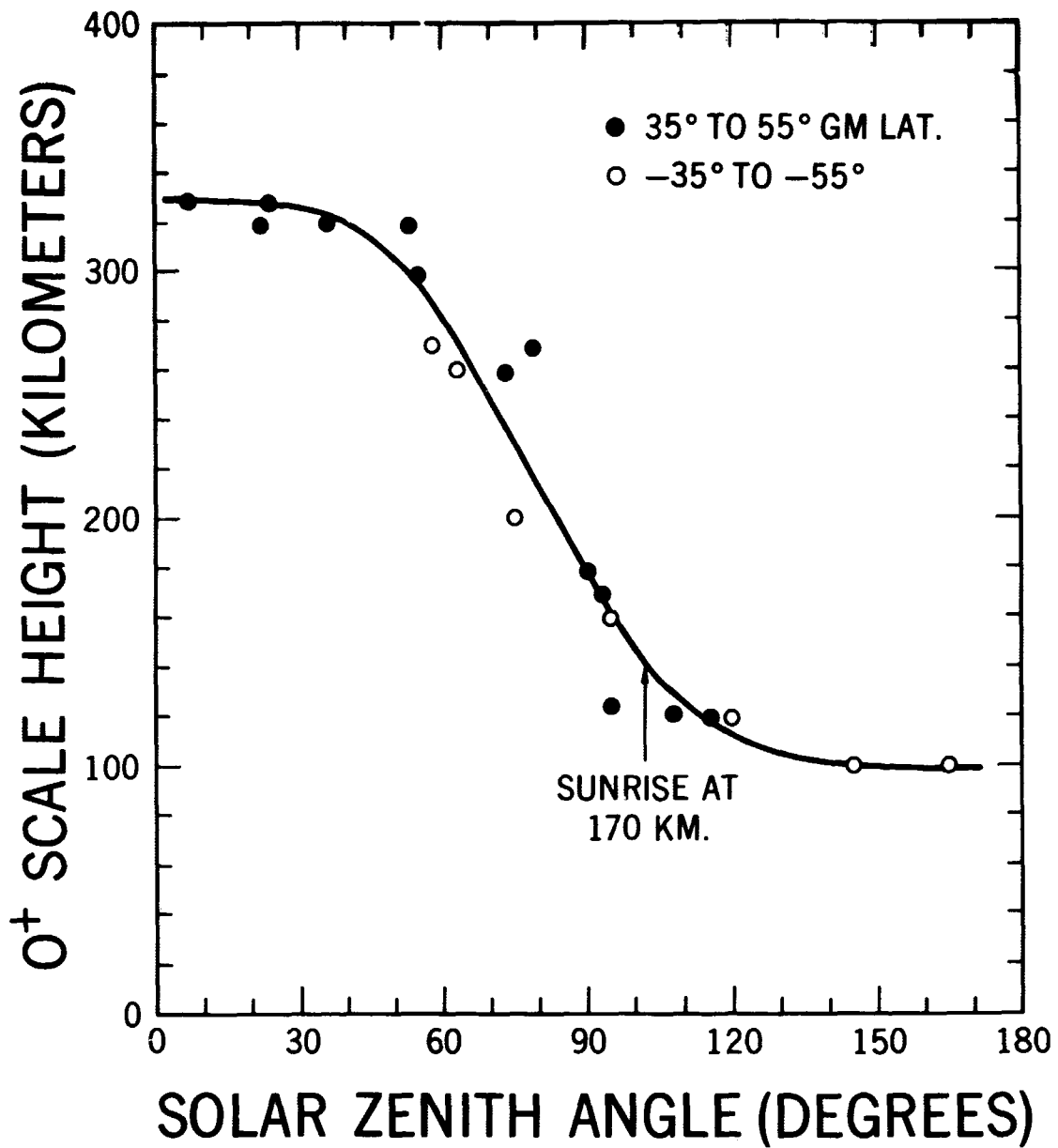


Figure 10. Relationship between solar zenith angle and observed O<sup>+</sup> scale height at midlatitudes in summer (northern) and winter (southern) hemispheres; applies to altitude range 1000-1500 km and local time interval 0000-1200 hr.